Nigerian Journal of Technology (NIJOTECH)
Vol. 44, No. 4, December, 2025, pp. 533-546
www.nijotech.com

Print ISSN: 0331-8443
Electronic ISSN: 2467-8821
https://doi.org/10.4314/njt.2025.5155

MACHINE LEARNING CLASSIFICATION TECHNIQUES TO PREDICT IN SITU COMPRESSIVE STRENGTH OF REINFORCED CONCRETE USING NDT DATA

AUTHORS:
B. Tekwani*, and A. B. Gupta

AFFILIATIONS:
Department of Structural Engineering, MBM University, Jodhpur, Rajasthan, India.

***CORRESPONDING AUTHOR:**
Email: bhartit.phdse@mbm.ac.in

ARTICLE HISTORY:
Received: June 06, 2025
Revised: September 15, 2025.
Accepted: September 25, 2025
Published: January 03, 2026.

KEYWORDS:
Classification Techniques; Compressive Strength; Schmidt Rebound Hammer; Steel Reinforced Concrete; Ultrasonic Pulse Velocity.

ARTICLE INCLUDES:
Peer review

DATA AVAILABILITY:
On request from author(s)

EDITORS:
Chidozie Charles Nnaji

FUNDING:
None

Abstract

Steel Reinforced Concrete (RC) is widely used in the construction industry due to its effective compressive and tensile strengths. This composite nature allows for withstanding diverse loading conditions. Assessing the structural condition of RC is essential for determining the extent of repair and retrofitting required for aged structures. Non-destructive testing (NDT) methods are commonly employed for this purpose. The objective of this study is to develop suitable correlations between compressive strengths of RC (f_{RC}) and results obtained from two ND Tests - Schmidt rebound hammer (R_S) test and Ultrasonic pulse velocity (V) test using machine learning techniques (ML) on the software platform of MATLAB. The experimental program involved casting 450 RC specimens, which included beam specimens with dimensions 70 cm × 15 cm × 15 cm and standard cube specimens with dimensions 15 cm × 15 cm × 15 cm, using concrete grades ranging from M25 to M35. The beams were reinforced with 2.68% longitudinal steel and provided with nominal concrete covers of 20 mm and 40 mm. NDT measurements (R_S and V) were taken on the beam specimens, while compressive strength was determined from the companion cube specimens via destructive compression testing. The collected data were then analyzed using MATLAB's Classification Learner app. A Support Vector Machine (SVM) model was used to establish the correlation between R_S and f_{RC}, while a Decision Tree classifier refined the V dataset with an accuracy of 99%. Using the ML approach, the data were effectively segregated through the developed models, which were further utilized to estimate the actual compressive strength of RC from NDT results. The study demonstrates that ML-based models can reliably estimate in-situ compressive strength from NDT results, yielding a practical approach for structural health assessment of RC.

1.0 INTRODUCTION

Over the last four decades, researchers have been working on establishing strength correlations of conventional concrete using NDT methods, particularly the R_S test and V test. With the growing use of Steel Reinforced Concrete (RC), it has become equally important to develop reliable assessment techniques for evaluating construction quality. In recent years, the integration of NDT with data-driven predictive approaches such as regression models and ML algorithms has been increasingly explored to improve the accuracy and efficiency of evaluations. The necessary corrections are required due to the presence of reinforcement (Table 1). True R_S and V readings are estimated by multiplying the measured value by appropriate correction factors.

HOW TO CITE:
Tekwani, B., and Gupta, A. B. "Machine Learning Classification Techniques To Predict *In* Situ Compressive Strength of Reinforced Concrete Using Ndt Data", *Nigerian Journal of Technology*, 2025; 44(4), pp 533-546, https://doi.org/10.4314/njt.2025.5155

The readings of V in the presence of reinforcement bars within concrete are higher than those in plain concrete [2]. As V waves partially travel through the reinforcement in RC structures, the measured velocity is higher, leading to inaccurate quality assessments of concrete based on these values. Plain concrete cubes measuring 150 mm × 150 mm × 150 mm and RC beams measuring 700 mm × 150 mm × 150 mm with reinforcement percentages of 0.8%, 1.0%, 1.2%, and 1.4% respectively, were tested using V instruments. Results showed that V values in reinforced samples were 6–14% higher than in plain concrete [3]. Since steel is much denser than concrete, the corresponding V values are expected to be higher. In an infinite steel medium, the V is typically around 5.90 km/s [4]. With the presence of steel reinforcement, the R_S test yields higher rebound numbers than on unreinforced surfaces, potentially differing by 8-12 points [27]. R_S and V readings were reduced by 9.4% and 8.1% respectively, under 80% compression stress applied to cubes. These values decreased by 2.5% and 1.4% respectively, under 80% flexural load on the RC beam. [27]Statistical models are developed nowadays using ML-AI techniques in which models learn from supervised or unsupervised data and predict the responses. The data-centric correlation equations were derived by Rathod et al. [5] from experimental results obtained using five different NDT methods, namely ground penetrating radar, half-cell potential (HCP), electric resistivity, infrared thermography, and V test. The study gave 2-dimensional contour and intensity maps to visualize and compare damage detection capabilities.

In 2024, the Flying NDT system made a significant advancement in autonomous SCA, especially in hard-to-reach areas. The developed robotic system addresses this by performing contact-based NDT using a hexacopter drone, integrated with two specialized sensors. A point sensor contains HCP, and electrical resistivity measurements were made using a two-point setup. A combined rolling sensor that incorporates a wheel-base system for simultaneous HCP and resistivity measurement via a four-point Schlumberger method was used. The sensor enabled the detection of chloride-induced corrosion before any visible sign appeared, thereby enhancing maintenance planning and structural safety [6].

Table 1: Empirical mathematical models suggested by various researchers for reinforced concrete using destructive and NDT tests

Reference	Regression Equation	Influencing Factors
[7]	$f = 0.677e^{0.00009v}$ $f = 1.4832R_S - 14.608, R^2 = 0.9715$	Reinforced concrete M25, M35, M45 MPa
[8]	$f = 23.76e^{0.2142v}, R^2 = 0.88$ $f = 0.0115{R_S}^2 + 0.8554R_S - 12.701, R^2 = 0.989$	Prototype RC wall 48 MPa strength with construction defects such as Honeycombing, delamination, and voids.

Although correlation models are readily available for determining the compressive strength of conventional plain concrete using NDT, they should not be directly applied to RC if the concrete cover is less. The presence of embedded steel reinforcement apparently increases the Rs and V values for RC when readings are taken at reinforced spots in comparison to those taken at unreinforced regions, thus falsely yielding higher values of strength. This discrepancy arises due to the significant difference in material densities. The density of steel bars is approximately 78.5 kN/m³, which is significantly higher than that of plain concrete, at 24 kN/m³. In such a case, using available equations of R_s and V, the estimated compressive strengths of RC (f_{RC}) may appear apparently higher than the actual strength. Therefore, correction factors must be applied to adjust the measured R_S and V values, ensuring they more accurately reflect true readings by accounting for the effects of reinforcement. These correction factors can be avoided if there is a way to segregate the readings taken on reinforced spots so that they can be discarded from the total number of readings.

The objective of this study is to establish a correlation between the compressive strength of RC and the results obtained from two NDT techniques: the R_S test and the V test, along with destructive compression testing. The M25–M35 range was selected because it represents the most widely used

https://doi.org/10.4314/njt.2025.5155

strength class for reinforced concrete slabs, beams, columns, and other moderately loaded structural elements. Cover depth has a significant influence on corrosion protection, thermal resistance, bond characteristics, and the effective stress distribution around reinforcement. The two cover values chosen represent two practical and contrasting conditions: 20 mm simulates typical minimum covers used for internal members or slabs where exposure is mild; 40 mm represents a conservative cover used for elements exposed to aggressive environments in columns and beam members, and for larger members where greater cover is needed for anchorage and corrosion allowance. Selecting these two discrete values enables assessment of how cover depth affects the accuracy and sensitivity of NDT techniques and strength-prediction models as cover alters both wave propagation and surface hardness readings. NDT instruments were operated at the reinforced spot and unreinforced spot of the same specimen for segregating true-false readings. Accordingly, this study aims to perform classification and regression analysis using both destructive test data and NDT values for RC, to distinguish between true and false values of R_S and V without relying on correction factors. Machine Learning (ML) algorithms implemented in MATLAB were used for this purpose.

2.0 MATERIALS, MIX DESIGN, AND DATA COLLECTION

2.1 Material and Experimental Program

The materials were selected according to Table 2, and mixes were prepared as outlined in Table 3. The mix design Table 3 for concrete grades M25, M30, and M35 according to the guidelines of IS 10262:2019 [11] and IS 456:2000 [12].

Table 2: Materials used for the mix design

Material	Source	Specific Gravity	Reference
Cement	Ultra-tech PPC 43 Grade	2.86	[9]
Sand	River sand procured from the local market, Zone II	2.44	Table 9 [10]
Coarse Aggregate	Kakani quarry, Jodhpur, Rajasthan, India	2.65	Table 7 [10]

Table 3: Mix design of conventional concrete per/ m^3

Material	M 25 Quantity (Kg/m^3)	M 30 Quantity (Kg/m^3)	M 35 Quantity (Kg/m^3)
Water	176.4	176.4	176.4
Cement	392	420	441
Chemical Admixture	3.92	4.2	4.41
Fine Aggregate	561	575	582
Coarse Aggregate (20 mm)	679	696	678
Coarse Aggregate (10 mm)	452	464	478
Adopted Mix Ratio	0.45:1:1.43:288	0.42:1:1.37:2.76	0.40:1:1.32:2.62

3.0 METHODOLOGY

The NDT and destructive test procedures performed on RC elements, covering the R_S test, V test, and compressive strength testing on companion cubes. The R_S tests, shown in Figure 2(a), conducted as per IS 516: Part 5/Sec 4–2020, provided true (T) values of rebound number ranges of 25–30, 30–35, and 35–41 for M25, M30, and M35 grades, respectively, when tested on plain concrete cubes (table 6).

The V tests, carried out using the direct transmission method as per IS 516: Part 5/Sec 1–2018, indicated true (T) velocities of 3.26 km/s, 3.86 km/s, and 3.95 km/s for M25, M30, and M35 grades, respectively,

when tested on plain concrete beams. Destructive compressive strength tests were performed on companion cube specimens at 28 days to validate NDT results, as shown in Figure (d).

Table 7 (a) summarizes 450 datasets obtained from R_S tests on RC beams with 20 mm and 40 mm cover depths, along with corresponding destructive test results on cube specimens, providing a comprehensive database for correlation analysis. In

https://doi.org/10.4314/njt.2025.5155

this dataset, 'R_S' denotes the rebound hammer reading taken on the RC beams; 'f_{RC}' represents the corresponding compressive strength.

Table 4: Casting details of beam and cube specimens

Parameter	**Details**
Total specimens cast	450 beams and 450 companion cubes
Beam dimensions	700 mm × 150 mm × 150 mm
Cube dimensions	15 cm × 15 cm
Reinforcement bar length	650 mm
Reinforcement ratio (Ast/Ac)	2.68% (Refer to Table 5)
Clear cover (bottom/side)	20 mm and 40 mm (bottom), 25 mm (side)
Concrete cover block size	20 mm × 25 mm × 40 mm
Mix design	As per Table 3
Casting method	Concrete poured in 3 layers, compacted by 35 strokes per layer (tamping rod)
Standard followed for compaction and curing	IS 1199 Part-5 [13]
Vibration	10–15 seconds using a handheld concrete vibrator
Surface finishing	Trowel finish
De-moulding time	24 hours after casting
Curing method	Wet curing by full water immersion
Curing duration & temperature	28 days at 27 ± 2°C

The true readings were taken from a concrete 15 cm^3 cube sample, which was placed in a compression testing machine (CTM) under a fixed load of 7 $N/mm^{2,}$ and R_S readings (horizontal in direction) were taken on surfaces (Figure 2(a)). Nine readings were taken on each of two opposite vertical faces accessible in CTM. While the false readings correspond to RC beams (Figure 2(b)), where the presence of reinforcement alters the rebound reading, 'D' is the decision factor used to segregate true (T) and false (F) rebound values for improved correlation accuracy.

Table 5: RC reinforcement detail

Type	HYSD
Elastic limit (MPa)	500
Φ (mm)	16
Number	3
A_{st} (cm^2)	6.03
A_c (cm^2)	225
A_{st}/ A_c (%)	2.68

https://doi.org/10.4314/njt.2025.5155

Table 6: Summary of NDT and DT procedures and results for RC elements

Test Name	Procedure/ Details	Concrete Grade	Actual Result Range/Avg.
R_S Test as per IS 516: Part 5 / Sec 4 – 2020 [15]	N-type R_S with 2.207 N-m impact energy. The Rebound Hammer is applied horizontally on beams for consistent results. Additional tests on cubes of the same grade for more accuracy.	M25 M30 M35	25–30 30–35 35–41
V Test as per IS 516: Part 5 / Sec 1 – 2018 [16]	The direct transmission method is used for pulse velocity. Ensures maximum energy transfer and precision. Evaluates internal quality and homogeneity of concrete.	M25 M30 M35	3.26 km/s 3.86 km/s 3.95 km/s
Compressive Strength Test as per IS 516: 2021 [14]	Carried out on all cube specimens at 28 days of curing. Using a calibrated compression testing machine	M25 M30 M35	Values compared with NDT results; not explicitly listed

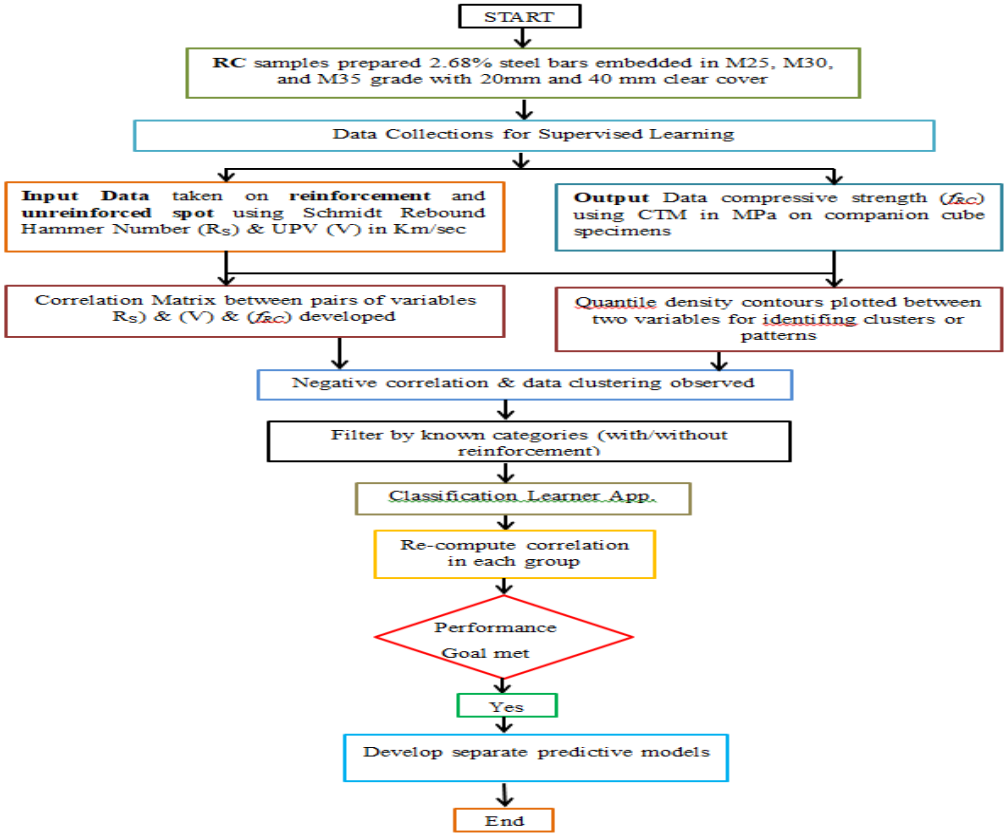

Figure 1: Experiment work processing steps

3.1 Data Collection

In the dataset represented in Table 7 (b), V denotes the measured pulse velocity values, f_{RC} represents the compressive strength determined from cube testing, and D is the decision factor used to distinguish between true and false readings. The true readings are taken from plain concrete beams, while the false readings correspond to RC beams, where the presence of reinforcement alters the pulse transmission. This distinction allows the

https://doi.org/10.4314/njt.2025.5155

reinforcement effect to be incorporated into the correlation analysis, thereby improving the accuracy of strength prediction models.

Table 7(a): 450 Data sets using the R_S test performed on the RC section at a depth of 20mm and 40 mm cover, and destructive test on cubes

R_S	f_{RC}	D	R_S	f_{RC}	D	R_S	f_{RC}	D
35	23.36	F	27.22	23.74	T	39.00	35.401	T
35	23.37	F	27.22	23.80	T	47.00	35.402	F
35	23.38	F	27.22	23.87	T	40.00	35.405	T
35	23.45	F	27.23	23.93	T	36.95	35.417	T
35	23.45	F	28.64	24.01	T	47.00	35.515	F
35	23.10	F	28.65	24.02	T	47.00	35.558	F
35	23.14	F	28.69	24.05	T	35.00	35.587	T
37	25.48	F	30.50	25.87	T	35.82	35.599	T
35	24.77	F	25.00	25.93	T	36.25	35.749	T
35	24.78	F	25.85	25.98	T	37.00	35.785	T
35	24.81	F	26.35	26.02	T	45.00	35.813	F
32.61	27.28	T	27.00	26.02	T	48.00	35.814	F
32.65	27.57	T	26.00	23.07	T	47.00	35.832	F
32.71	27.82	T	30.00	23.07	T	44.00	35.842	F
32.72	27.83	T	28.69	24.11	T	37.85	35.844	T
32.73	27.86	T	28.72	24.13	T	39.00	35.844	T
32.73	27.86	T	29.00	23.20	T	45.00	35.862	F
32.75	28.09	T	30.00	23.24	T	38.22	35.989	T
32.80	28.23	T	30.45	23.25	T	35.00	35.989	T
22.98	23.21	T	30.36	23.26	T	36.12	36.062	T
:	:	:	:	:	:	:	:	:
:	:	:	:	:	:	:	:	:
30.36	23.26	T	29.00	23.10	T	32	29.32	T
29.25	23.36	T	28.65	23.14	T	36	34.00	T
29.15	23.37	T	26.00	25.48	T	40	38.81	T
28.47	23.38	T	30.51	24.77	T	39	36.60	T

Figure 2(a): R_S test performed on cube specimen

Figure 2(b): R_S test performed at the location of the bar

https://doi.org/10.4314/njt.2025.5155

Table 7 (b): 450 Data sets using the V test performed on the RC section at depths of 20mm and 40 mm cover, and Destructive test on cubes

V	f_{RC}	D	V	f_{RC}	D	V	f_{RC}	D
3.44	27.28	F	3.59	26.02	F	3.58	24.76	F
3.44	27.57	F	3.59	23.07	F	3.28	23.50	T
3.44	27.82	F	3.59	23.07	F	3.30	23.54	T
3.44	27.83	F	3.60	24.11	F	3.31	23.55	T
3.44	27.86	F	3.60	24.13	F	3.31	23.55	T
3.45	27.86	F	3.60	23.20	F	3.33	23.58	F
3.45	28.09	F	3.60	23.24	F	3.34	23.60	F
3.46	28.23	F	3.61	23.25	F	3.34	23.62	F
3.46	23.21	F	3.61	23.26	F	3.36	23.74	F
3.46	23.58	F	3.61	23.36	F	3.36	23.80	F
3.48	23.70	F	3.61	23.37	F	3.37	23.87	F
3.51	23.73	F	3.62	23.38	F	3.37	23.93	F
3.51	24.26	F	3.62	23.45	F	3.37	24.01	F
3.35	24.56	F	3.62	23.45	F	3.37	24.02	F
3.24	24.59	F	3.62	23.10	F	3.37	24.05	F
3.24	24.79	F	3.64	23.14	F	3.17	25.87	T
3.25	24.80	F	3.64	25.48	F	3.18	25.93	T
3.25	24.82	F	3.66	24.77	F	3.18	25.98	T
3.25	25.00	F	3.66	24.78	F	3.18	26.02	T
3.25	25.18	F	3.66	24.81	F	3.18	26.02	T
:	:	:	:	:	:	:	:	:
:	:	:	:	:	:	:	:	:
5.21	37.430	F	5.52	39.063	F	3.778	39.17	T
3.66	37.455	T	5.52	39.068	F	3.780	39.21	T
5.23	37.471	F	5.52	39.089	F	3.784	39.32	T
3.98	37.475	T	5.81	32.74	F	3.789	39.32	T

Figure 2(c): V test performed on RC beam at the location of the bar

Figure 2(d): Destructive Test on companion Cube

Table 8: Descriptive range of data for ANN training and testing

Variable	Mean	Median	Mode	SD	Range	Min	Max
R_S	36.12	35	35	7.76	33	22	55
V(km/sec)	4.16	3.80	3.53	0.87	2.89	3.10	6
f_{RC} (MPa)	30.57	29.23	25.48	5.98	17.98	22	39.95

https://doi.org/10.4314/njt.2025.5155

3.2 Correlation Matrix

Table 9 shows the data of the correlation matrix between variables. The correlation matrix data helps us determine whether linear regression is suitable for deriving the relationships, or advanced machine learning techniques must be applied to achieve non-linear correlations. The correlation results reveal a strong relationship between rebound number and compressive strength (R2 = 0.773), indicating that higher Rs values generally correspond to higher strength. In contrast, ultrasonic pulse velocity exhibits negligible correlation with both Rs (R2 = -0.07128) and f (R2 = -0.02793), indicating minimal linear association.

Table 9: Correlation matrix of variables

Variables	R_s	F	V
R_s	1		
f	0.773063	1	
V	-0.07128	-0.02793	1

3.3 Quantile Density Contours

The quantile density contours were plotted for a certain range of the data set, and the results were explained.

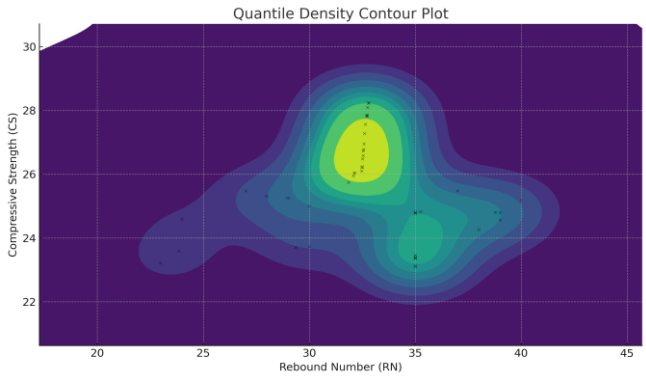

Figure 3 (a): Quantile Density Contours

The contour zones illustrate good correlation between NDT and compressive strength values. The data density with the highest concentration observed R_s equal to 30–33 and compressive strength 25–27 MPa. Yellow/green areas indicate high clustering; while blue/purple regions show lower density resign.

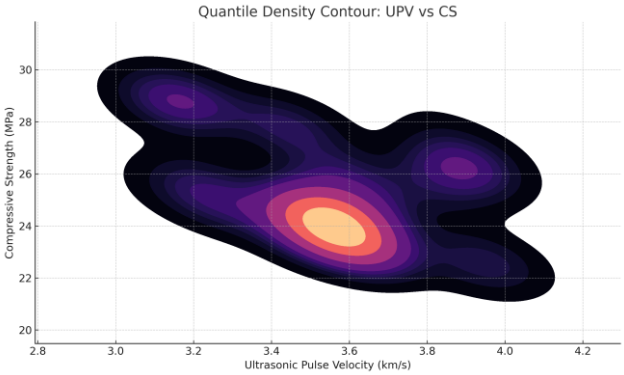

Figure 3 (b): Quantile Density Contours

Figure 3(b) Quantile density contour plot showing the relationship between V test and Compressive Strength for a certain range of the dataset. The color gradient represents data density, with yellow–orange zones indicating the highest concentration of data points and purple–black zones showing progressively lower densities. The densest cluster lies around V = 3.4–3.6 km/s and CS = 23–25 MPa, representing the strongest correlation zone. The spread of contours towards higher UPV (up to ~ 4.0 km/s) and CS (~30 MPa) reflects data variability caused by the influence of reinforcement and material heterogeneity. This visualization confirms that V is a reliable indicator of CS within certain ranges, while corrections are required for reinforced sections.

3.4 Statistical Model Development: Classification Techniques

The target variable f_{RC} is continuous; however, it is important to note that classification techniques were applied to the R_S and V values to categorize them into discrete levels or classes as part of the analysis.

The data shown in Table 7(a) and Table 7(b) were separately inserted into the classification learner application [26]. To assess the model's performance and generalization ability, 5-fold cross-validation was used. In the study, the dataset was divided into 70% for training, 15% for validation, and 15% for testing. Additionally, we employed 5-fold cross-validation to ensure robustness and to enhance the generalizability of the machine learning models. This process divides the dataset into five subsets, training the model on four and validating it on the fifth in a rotating fashion. Once the data is loaded, users can split it into training and validation sets and perform cross-validation to prevent over-fitting.

https://doi.org/10.4314/njt.2025.5155

4.0 RESULTS AND DISCUSSION

After training, the Classification Learner app displays key performance metrics, including accuracy, precision, recall, and F1-score. The best-performing model can be exported as a MATLAB function or a trained model structure for further use in scripting and deployment.

Confusion matrices were determined for both models. From Table 10, it is observed that the SVM model achieved the highest validation accuracy of 99.35% for R_S data, Figure 4 demonstrate that the classifier achieved for class 'T' 99.7% positive predictive value (PPV) and 100% true positive rate (TPR) with only a negligible 0.3% false discovery rate (FDR). Such minimal error is consistent with experimental noise or local heterogeneities in concrete (presence of reinforcement). Similarly Figure 5, decision tress outperformed with an accuracy of 99.45% for V data.

Class 'T' achieved a 95.5% TPR and 92.8% PPV, with only a 1.9% misclassification rate into class F. The false discovery rate for class T was 7.2%, slightly higher than for the other categories, suggesting some overlap in model prediction between F and T values. These small errors were occurred due to microstructural variation, reinforcement interference or signal scattering near cracks or voids.

Table 10: Percentage Accuracy of validation obtained for all models in the classification learner application

Model Number	Model Type	Status	Accuracy (%)
1	"Decision Tree (DT)" (V)	"Trained"	99.45
2.2	"Efficient Linear SVM" (R_S)	"Trained"	99.35

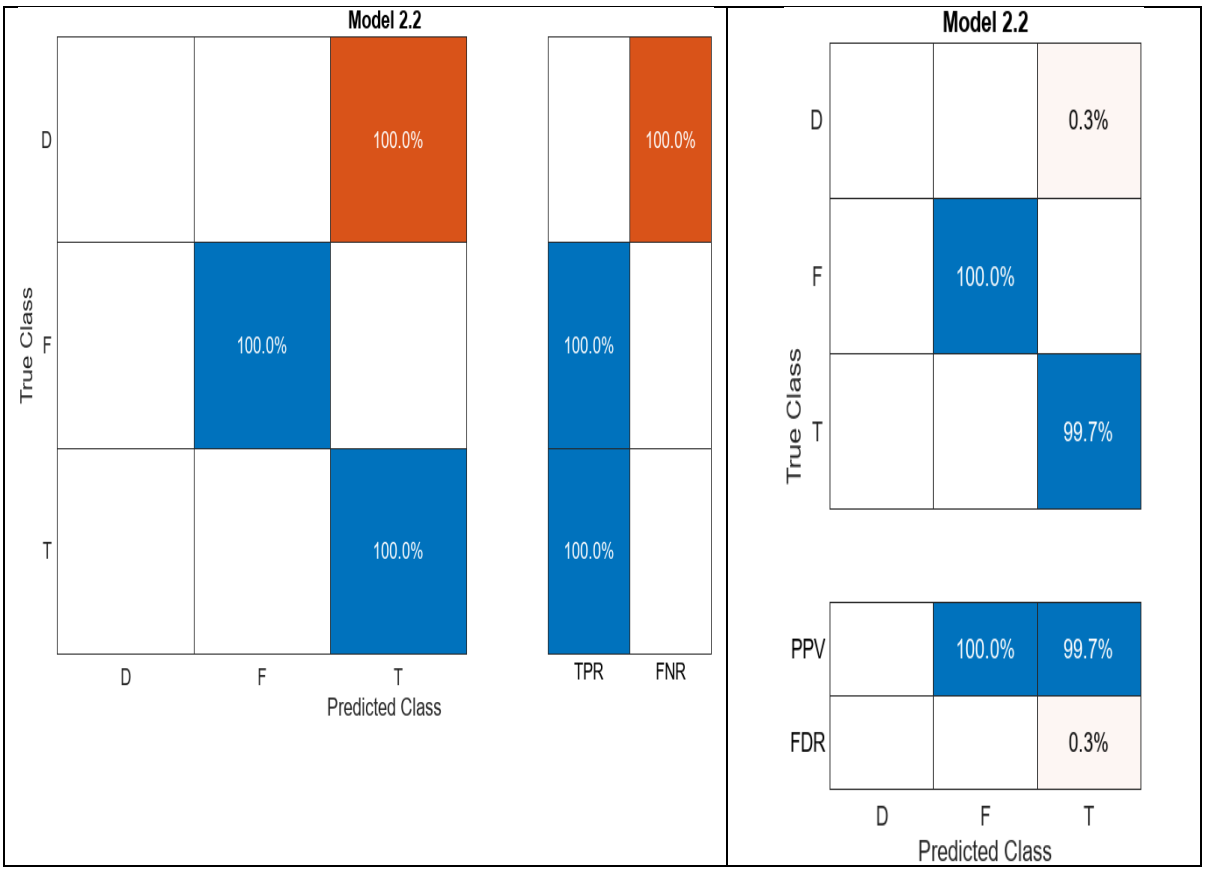

Figure 4: Confusion Matrix from MATLAB 2023b for a successfully SVM-trained model

https://doi.org/10.4314/njt.2025.5155

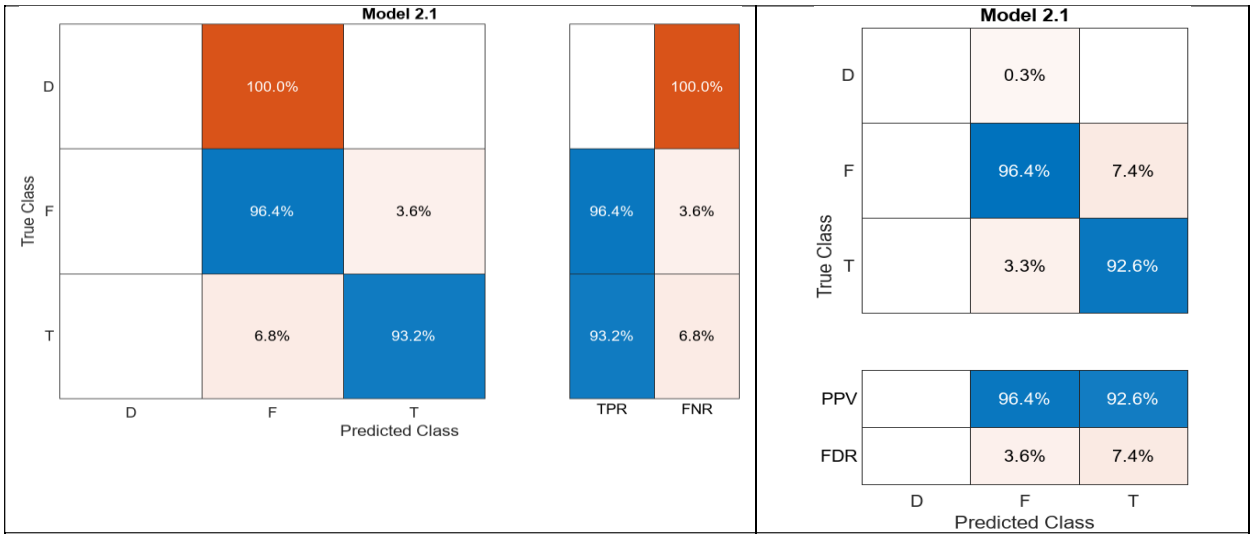

Figure 5: Confusion Matrix from a Successfully DT-trained model using V-f_{RC} Data

4.1 Svm-Based Equation For Predicting The Compressive Strength of Rc from Rebound Number

The RC data set is imported into the classification learner application, where R_S and f_{RC} are the predictor variables, and data is the categorical response variable with two possible classes: 'T' and 'F'.

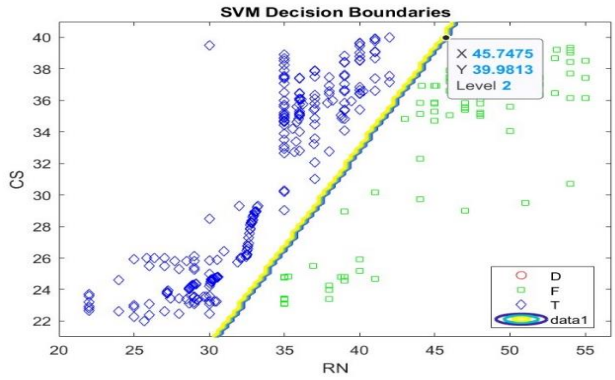

Figure 6: Decision boundary using SVM classifier, MATLAB

The decision regions are then plotted using the contour function over a scatter plot of the original data, highlighting the separation between different classes. Additionally, the script extracts the decision boundary equations (Figure 6) for each binary classifier by retrieving the weight vector (w^T) and bias (b) from the trained SVM learners [29], providing analytical insight into the classification rules.

Figure 7 explains the SVM decision boundary plot between Rebound Number and Compressive Strength. The yellow line represents the linear boundary separating true (green squares) and false (blue diamonds) rebound values. Data to the right of the boundary are classified as true readings, while those on the left are false, indicating the influence of reinforcement. This separation enhances the reliability of compressive strength prediction for RC using rebound hammer data.

Once data is trained, a linear SVM provides a decision boundary equation in the form:

$$w_1 x_1 + w_2 x_2 + b = 0 \quad (1)$$

The decision boundary effectively refines the R_S data, and with the help of equation (1), the equation of true f_{RC} using R_s data is determined, and the final result is given by Equation (3).

$w_1 = 1.587, w_2 = -1.00009$; b = -23 obtained from MATLAB 2023b Simulink, put these values in equation (2)

$$f_{SRC} = -\frac{Beta\ value\ 1}{Beta\ value2} R_S - \frac{bias}{Beta\ value2} \quad (2)$$

$$f_{SRC} = 1.587 R_S - 23 \quad (3)$$

4.2 Decision Tree (DT) Analysis of The Relationship Between Compressive Strength and Ultrasonic Pulse Velocity (UPV)

https://doi.org/10.4314/njt.2025.5155

In this study, a DT classifier [29] was developed using the Classification and Regression Tree (CART) algorithm, with the Gini Index employed as the splitting criterion. The results demonstrated that the DT classifier achieved the highest accuracy in predicting V outcomes across different concrete grades (Figure 7).

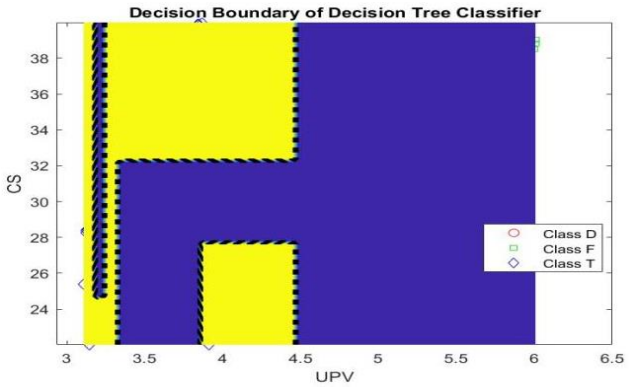

Figure 7: Decision boundary plot for V RC data set using DT

4.3 Error Matrices Developed for The Classification Model Using Confusion Matrices:

A 3×3 confusion matrix [25, 29] is constructed for the models that achieve the highest accuracy, with the true class on one axis and the predicted class on the other. This matrix is developed for a binary classification problem using the Classification Learner application in MATLAB. Error matrices [30] are evaluated using all the formulae discussed in Table 11.

The ML models achieved high accuracy in predicting (fRC). There are no previous studies that have reported an ML-based interpretation of combined NDT data for this purpose. Therefore, direct comparison with published work is not possible; instead, our findings establish an initial benchmark and are contrasted with related studies using NDT techniques or conventional statistical correlations, which provide higher prediction errors.

A key limitation of the present work is that the study is based on lab-controlled specimens, which may not fully capture field influences such as material variability, workmanship, and environmental exposure.

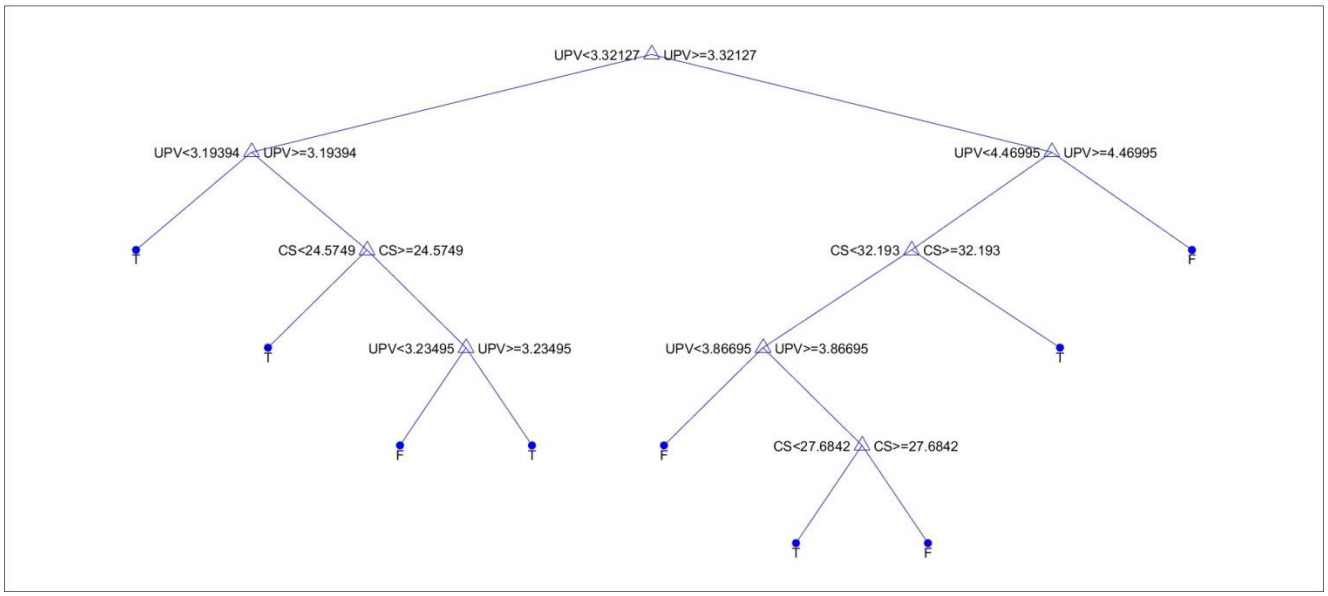

Figure 8: RC Sample Decision Tree of V data set

Table 11: Performance of Error Matrices using the Confusion Matrix

Errors	Linear SVM RC (R_S v/s f)	DT Classifier RC(V v/s f)

https://doi.org/10.4314/njt.2025.5155

$Precision = \frac{TP}{TP + FP}$	1	0.978
$FDR = 1 - Precision = 1 - \frac{TP}{TP + FP}$	0	0.022
$Recall = \frac{TP}{TP + FN}$	1	0.995
$FNR = 1 - Recall = 1 - \frac{TP}{TP + FN}$	0	0.045
$F1\,score = \frac{2}{\frac{1}{Precision} + \frac{1}{Recall}}$	1	0.98

5.0 CONCLUSIONS

The obtained NDT dataset using R_S test and V test values for RC, when analyzed through a correlation matrix, revealed a weak correlation between the data. The density contours also supported this observation, for a certain range of the dataset. Therefore, it

becomes necessary to segregate or filter the NDT data values to determine the correct compressive strength of the specimens.

R_S tests were conducted on reinforced and unreinforced regions of all beams with compressive strengths ranging from 25 MPa to 35 MPa. To ensure accurate R_S measurements, concrete cubes of the same grade were cast. The tests yielded corrected R_S values of ranges between 25-30 for M25 grade concrete, 30-35 for M30 grade, and 35-41 for M35 grade.

The SVM model effectively established a clear decision boundary between rebound number and compressive strength CS, enabling accurate classification of RC specimens into strength categories. The nearly linear separation highlights the robustness of SVM in handling nonlinear yet separable data, minimizing misclassification and improving prediction reliability. Equation (3) obtained from the SVM classifier model effectively predicts the in-situ strength of RC members for concrete grades M25-M35 using rebound number values.

The presence of a steel bar affects the transit time between transducers because the V in steel is higher than in concrete. If there is a path through the steel bar that allows the wave to reach the receiver more quickly, it highlights the influence of the steel bar on the measured transit time. The V in plain concrete is generally expected to remain consistent regardless of the transducer location along the beam. However, it was observed from readings that the average V tends to decrease as the spacing between transducers increases, as shown in Figure 2(b).

To obtain the most accurate V measurement, resulting in a V of 3.26 Km/s for M25 grade, 3.56 Km/s for M30, and 3.95 Km/s for M35. However, the influence of the reinforcement bars significantly affected the measurements, making the direct interpretation of the concrete properties unsuitable without accounting for the impact of reinforcement.

By employing MATLAB's Classification Learner, a Decision Tree Classifier was developed that successfully segregated V values into true and false categories with an overall accuracy of 99%. The classification tree effectively analyzed V values and categorized them based on concrete strength grades:
M25 Grade Concrete: V ranges from 3.23 km/sec to 3.8 km/sec. M30 Grade Concrete: V falls within 4.0 km/sec to 4.5 km/sec. M35 Grade Concrete: V should ideally be less than 4.7 km/sec.

The percentage change in V observed for specimens reinforced with 16mm φ steel bars was 15%, 12% and 16% for beams M25C20, M30C20, and M35C20, respectively, when compared with the plain concrete specimen. This variation reflects the combined influence of both the higher concrete grade and the reinforcement positioned beneath. However, in the R_S values, no significant change is noted due to the reinforcement placed at a depth of 40mm.

https://doi.org/10.4314/njt.2025.5155

Future work could enhance the study by employing deep- learning techniques to capture complex patterns, expending dataset with measurements from actual field conditions, and investigating the influence of higher reinforcement ratios using hybrid NDT techniques.

REFERENCES

[1] Alwash, M., Breysse, D., and Sbartai, Z. M., "Non-destructive strength evaluation of concrete: Analysis of some key factors using synthetic simulations", *Construction and Building Materials*, **99**: 235–245, 2015. https://doi.org/10.1016/j.conbuildmat.2015.09.014

[2] Panedpojaman, P., and Tonnayopas, D., "Rebound hammer test to estimate compressive strength of heat-exposed concrete", *Construction and Building Materials*, **172**: 387–395, 2018. https://doi.org/10.1016/j.conbuildmat.2018.03.236

[3] Mehta, P. K., and Monteiro, P. J. M., *Concrete: Microstructure, Properties, and Materials*, 4th ed., McGraw-Hill Education, New York, USA, 2014.

[4] Masi, A., Chiauzzi, L., and Manfredi, V., "Criteria for identifying concrete homogeneous areas for the estimation of in-situ strength in RC buildings", *Construction and Building Materials*, **121**: 576–587, 2016. https://doi.org/10.1016/j.conbuildmat.2016.06.014

[5] Rathod, H., and Gupta, R., "Two-dimensional non-destructive testing data maps for reinforced concrete slabs with simulated damage", *Data in Brief*, **25**: 104127, 2019. https://doi.org/10.1016/j.dib.2019.104127

[6] Pfändler, P., Bodie, K., Crotta, G., Pantic, M., Siegwart, R., and Angst, U., "Non-destructive corrosion inspection of reinforced concrete structures using an autonomous flying robot", *Automation in Construction*, **158**: 105241, 2024. https://doi.org/10.1016/j.autcon.2023.105241

[7] Kencanawati, N. N., Akmaluddin, Marlitasari, R., and Paedullah, G., "Study on robustness of rebound hammer and ultrasonic pulse velocity measurement in several concrete damage levels", *IOP Conference Series: Earth and Environmental Science*, **708**(1): 012012, 2021. https://doi.org/10.1088/1755-1315/708/1/012012

[8] Al-Neshawy, F., Ferreira, M., and Puttonen, J., "NDT assessment of a thick-walled reinforced concrete mock-up of NPP concrete structures", *Proceedings of NDT-CE 2022 - International Symposium on Nondestructive Testing in Civil Engineering*, Zurich, Switzerland, 2022.

[9] Bureau of Indian Standards (BIS), *IS 455:1989 – Portland Slag Cement—Specification (Fourth Revision)*, New Delhi, India: BIS, 1989.

[10] Bureau of Indian Standards (BIS), *IS 383:2016 – Specification for Coarse and Fine Aggregates for Concrete (Third Revision)*, New Delhi, India: BIS, 2016.

[11] Bureau of Indian Standards (BIS), *IS 10262:2019 – Concrete Mix Proportioning Guidelines (Second Revision)*, New Delhi, India: BIS, 2019.

[12] Bureau of Indian Standards (BIS), *IS 456:2000 – Plain and Reinforced Concrete – Code of Practice (Fourth Revision)*, New Delhi, India: BIS, 2000.

[13] Bureau of Indian Standards (BIS), *IS 1199 (Part 5):2018 – Fresh Concrete—Method of Sampling, Testing and Analysis, Part 5: Making and Curing of Test Specimens*, New Delhi, India: BIS, 2018.

[14] Bureau of Indian Standards (BIS), *IS 516 (Part 1):2021 – Testing of Strength of Hardened Concrete, Section 1: Compressive, Flexural and Split Tensile Strength*, New Delhi, India: BIS, 2021.

[15] Bureau of Indian Standards (BIS), *IS 516 (Part 5/Sec 4):2020 – Hardened Concrete – Methods of Test, Part 5: Non-destructive Testing of Concrete, Section 4: Rebound Hammer Test*, New Delhi, India: BIS, 2020.

[16] Bureau of Indian Standards (BIS), *IS 516 (Part 5/Sec 1):2018 – Hardened Concrete – Methods of Test, Part 5: Non-destructive Testing of Concrete, Section 1: Ultrasonic Pulse Velocity Test*, New Delhi, India: BIS, 2018.

[17] Cortes, C., and Vapnik, V., "Support vector networks", *Machine Learning*, **20**(3): 273–297, 1995. https://doi.org/10.1007/BF00994018

[18] Ng, A., *Machine Learning Notes*, Stanford University, 2023. https://stanford.edu/materials/aimlcs229/cs229-notes1.pdf

[19] Zhang, T., and Zhou, Z.-H., "Optimal margin distribution machine", *arXiv preprint*,

https://doi.org/10.4314/njt.2025.5155

arXiv:1604.03348, 2016. https://arxiv.org/abs/1604.03348

[20] Goodfellow, I., Bengio, Y., and Courville, A., *Deep Learning*, MIT Press, Cambridge, MA, USA, 2016. https://www.deeplearningbook.org

[21] Cristianini, N., and Shawe-Taylor, J., *An Introduction to Support Vector Machines and Other Kernel-based Learning Methods*, Cambridge University Press, Cambridge, UK, 2000. https://doi.org/10.1017/CBO9780511801389

[22] Fan, R.-E., Chang, K.-W., Hsieh, C.-J., Wang, X.-R., and Lin, C.-J., "LIBLINEAR: A library for large linear classification", *Journal of Machine Learning Research*, **9**: 1871–1874, 2008.

[23] Quinlan, J. R., "Induction of decision trees", *Machine Learning*, **1**(1): 81–106, 1986. https://doi.org/10.1007/BF00116251

[24] MathWorks, "Regression Learner App – Perform regression analysis using machine learning", *MATLAB Documentation*, The MathWorks, Inc., Natick, MA, USA, 2023. https://www.mathworks.com/help/stats/regression-learner-app.html

[25] Shirdel, M., Di Mauro, M., and Liotta, A., "Worthiness Benchmark: A novel concept for analyzing binary classification evaluation metrics", *Information Sciences*, **678**: 120882, 2024. https://doi.org/10.1016/j.ins.2024.120882

[26] MathWorks, "Classification Learner App – Train classification models to predict data", *MATLAB Documentation*, The MathWorks, Inc., Natick, MA, USA, 2023. https://www.mathworks.com/help/stats/classification-learner-app.html

[27] Bensaber, A., Boudaoud, Z., Toubal Seghir, N., Czarnecki, S., and Sadowski, Ł., "The assessment of concrete subjected to compressive and flexural preloading using nondestructive testing methods: Correlation between concrete strength and combined method (SonReb)", *Measurement*, **222**: 113659, 2023. https://doi.org/10.1016/j.measurement.2023.113659

[28] Agarwal, G., Tu, W., Sun, Y., and Kong, L., "Flexible quantile contour estimation for multivariate functional data: Beyond convexity", *Computational Statistics & Data Analysis*, **168**: 107400, 2022. https://doi.org/10.1016/j.csda.2021.107400

[29] Bayode, O., Aiyelokun, O., Osanyinlokun, O., and Adanikin, A., "Enhancing road crash prediction: A comparative study of machine learning algorithms and safety performance functions on the Lagos-Ibadan Expressway", *Nigerian Journal of Technology*, **44**(2): 215–221, 2025. https://doi.org/10.4314/njt.v44i2.5

[30] Omonayin, E., Akande, O. N., Muhammad, A., and Enemuo, S., "Evaluating deep learning models for real-time waste classification in smart IoT environment", *Nigerian Journal of Technology*, **44**(2): 357–366, 2025. https://doi.org/10.4314/njt.v44i2.18

https://doi.org/10.4314/njt.2025.5155